

Crystal structure of the human adenovirus proteinase with its 11 amino acid cofactor

Jianzhong Ding, William J. McGrath¹,
Robert M. Sweet¹ and Walter F. Mangel^{1,2}

Physics Department, State University of New York at Stony Brook,
Stony Brook, NY 11794-3800 and ¹Biology Department, Brookhaven
National Laboratory, Upton, NY 11973-5000, USA

²Corresponding author

J. Ding and W.J. McGrath contributed equally to this manuscript.

The three-dimensional structure of the human adenovirus-2 proteinase complexed with its 11 amino acid cofactor, pVIc, was determined at 2.6 Å resolution by X-ray crystallographic analysis. The fold of this protein has not been seen before. However, it represents an example of either subtly divergent or powerfully convergent evolution, because the active site contains a Cys-His-Glu triplet and oxyanion hole in an arrangement similar to that in papain. Thus, the adenovirus proteinase represents a new, fifth group of enzymes that contain catalytic triads. pVIc, which extends a β -sheet in the main chain, is distant from the active site, yet its binding increases the catalytic rate constant 300-fold for substrate hydrolysis. The structure reveals several potential targets for antiviral therapy.

Keywords: catalytic triad/convergent evolution/cysteine proteinase/peptide cofactor/viral proteinase

Introduction

Human adenovirus proteinase activity, like that of many virus-coded proteinases, is absolutely required for the synthesis of infectious virus (Weber, 1976). The proteinase probably acts in newly assembled virions where it cleaves multiple copies of six precursor proteins (Mirza and Weber, 1980; Hannan *et al.*, 1983). There are ~10 proteinase molecules per virion (Anderson, 1990), and they make about 2500 highly specific cleavages to render a virus particle infectious. A temperature-sensitive mutation in the proteinase activity was mapped to the L3 23K gene (Weber, 1976; Yeh-Kai *et al.*, 1983). Sequences of L3 23-kDa proteins from 12 different adenovirus serotypes show no homology to other protein sequences (Cai and Weber, 1993). The L3 23K gene has been cloned and expressed, and the resultant protein with 204 amino acid residues has been purified (Anderson, 1993; Tihanyi *et al.*, 1993; Webster *et al.*, 1993; Mangel *et al.*, 1996).

Recombinant adenovirus endoproteinase (AVP) has little activity compared with that in disrupted virions; this prompted a search for cofactors. One cofactor was found to be the 11 amino acid peptide, pVIc, from the C-terminus of the virion precursor protein pVI (Mangel *et al.*, 1993; Webster *et al.*, 1993). That peptide (GVQSLKRRRCF) binds in a 1:1 ratio to AVP with an apparent dissociation

constant, K_d , of 12 nM (McGrath *et al.*, 1996c). Another cofactor is the viral DNA (Mangel *et al.*, 1993), which exhibits a K_d with respect to adenovirus-2 (Ad2) DNA molecules of 7 pM (McGrath *et al.*, 1996c). The cofactors increase k_{cat} , the catalytic rate constant for substrate hydrolysis: 300-fold with pVIc and 6000-fold with both pVIc and Ad2 DNA (Mangel *et al.*, 1996).

One can suggest roles for the cofactors. The apoenzyme is relatively inactive before and during virion assembly so it will not cleave virion precursor proteins. Once virions are assembled, the proteinase encounters pVI and cuts out pVIc, which binds to the proteinase. The activated AVP-pVIc complex then uses the viral DNA as a guidewire and cofactor to cleave the remaining precursor proteins. To ascertain which residues are involved in catalysis, hence the class of the proteinase, and to determine the structural basis of substrate specificity and of cofactor activation of the enzyme, we have solved the three-dimensional structure of the AVP-pVIc complex by X-ray diffraction to a resolution of 2.6 Å.

Results

Quality of the model

The structure of the AVP-pVIc complex was solved with single-isomorphous replacement supplemented with anomalous scattering (Table I). The final model, refined against diffraction data measured from crystals of the native protein contained 1715 non-hydrogen protein atoms and 45 solvent molecules and gave a crystallographic R factor of 18.3% [$R_{free} = 23.3\%$; (Brünger, 1993)] for the data from 6 to 2.6 Å. The root mean square (r.m.s.) deviations are 0.008 Å from ideal bond lengths and 1.6° from ideal bond angles. The Ramachandran plot (Ramachandran and Sasisekharan, 1968) for the final model shows 85% of the residues in the most favored regions and none of the non-glycine residues in disallowed regions.

Table I. Summary of the structure determination

Resolution range	2.6–6.0 Å
Observations in refinement ^a	10473
Non-hydrogen protein atoms	1715
Solvent molecules	45
R_{corr} ^b	18.4%
R_{free} ^a	23.3%
r.m.s. deviations from ideal geometry ^c	bond angles (°) 1.6 bond lengths (Å) 0.008
Residues in most favorable region of Ramachandran plot ^d	85%

^a9% of the 11560 observations were sequestered at the beginning of the refinement for calculation of an unbiased R factor.

^b $R_{corr} = \Sigma |F_{obs} - F_{calc}| / \Sigma F_{obs}$

^cAs calculated by X-PLOR (Brünger, 1993).

^dAs calculated by PROCHECK (Laskowski *et al.*, 1993).

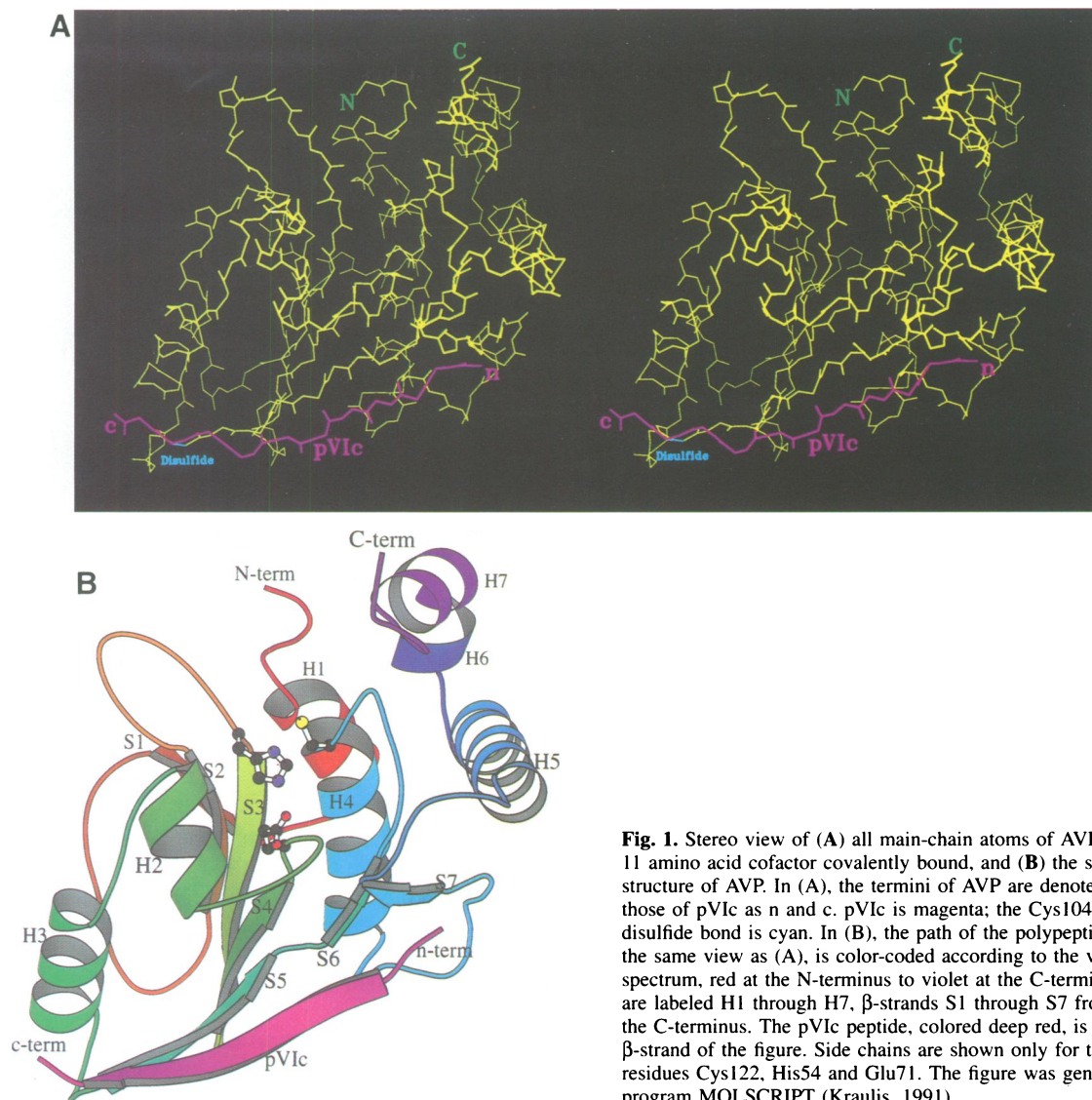


Fig. 1. Stereo view of (A) all main-chain atoms of AVP with its 11 amino acid cofactor covalently bound, and (B) the secondary structure of AVP. In (A), the termini of AVP are denoted as N and C, those of pVlc as n and c. pVlc is magenta; the Cys104-Cys10' disulfide bond is cyan. In (B), the path of the polypeptide, shown in the same view as (A), is color-coded according to the visible spectrum, red at the N-terminus to violet at the C-terminus. α -Helices are labeled H1 through H7, β -strands S1 through S7 from the N- to the C-terminus. The pVlc peptide, colored deep red, is the nearest β -strand of the figure. Side chains are shown only for the active-site residues Cys122, His54 and Glu71. The figure was generated with the program MOLSCRIPT (Kraulis, 1991).

Folding of the complex

The AVP-pVlc complex is ovoid (Figure 1A and B); three α -helices form the blunt end. In the central region are three α -helices which interact with a single β -sheet. A seventh helix is at the pointed end. The β -sheet, composed of five strands, separates the blunt from the pointed end. The cofactor pVlc becomes the sixth β -strand in the central β -sheet, forming both a disulfide bond and hydrogen bonds. Two small β -strands cross near the bottom of the central helix.

Binding of pVlc

Residues 1'-3' and 4'-11' of pVlc interact with two non-contiguous regions on AVP (Figure 2A). The first three bind strongly on or near β -strand S7. In forming the sixth (antiparallel) β -strand of the core of the structure, residues 4'-10' interact with S5, residues 104-109. Residue Cys10' forms a disulfide bond with Cys104 of AVP. In addition to the eight hydrogen bonds involved in formation of the β -sheet, there are five interactions (side-chain to side-chain) between pVlc and AVP. If pVlc acts as a cofactor by bringing together two non-contiguous regions of AVP, thereby altering the conformation of the active site to

increase k_{cat} , then a peptide with only pVlc residues 4'-11' may be an enzyme inhibitor and potential antiviral agent.

Possible DNA-binding sites

Four large clusters of positive charge lie on the surface of the molecule, ranging in area from 45 to 65 \AA^2 (Figure 2B). Some of these clusters may interact with the viral DNA in its role as a cofactor by providing non-specific binding sites for negatively charged phosphate groups on DNA. The shortest distances between these pairs of clusters, ~ 24 \AA , are commensurate with the rise of a single turn of double-stranded DNA.

Discovery of the active site

Comparison of AVP to all unique protein molecules in the Brookhaven Protein Data Bank (Bernstein *et al.*, 1977) with the program Dali (Holm and Sander, 1994) revealed no equivalent structure, suggesting that AVP represents a new family of protein molecules. Dali alignments require a sequential ordering of segments, so the program cannot locate other topological similarities. However, we noticed a helix and several β -strands within the central region that had similarities to both subtilisin and papain.

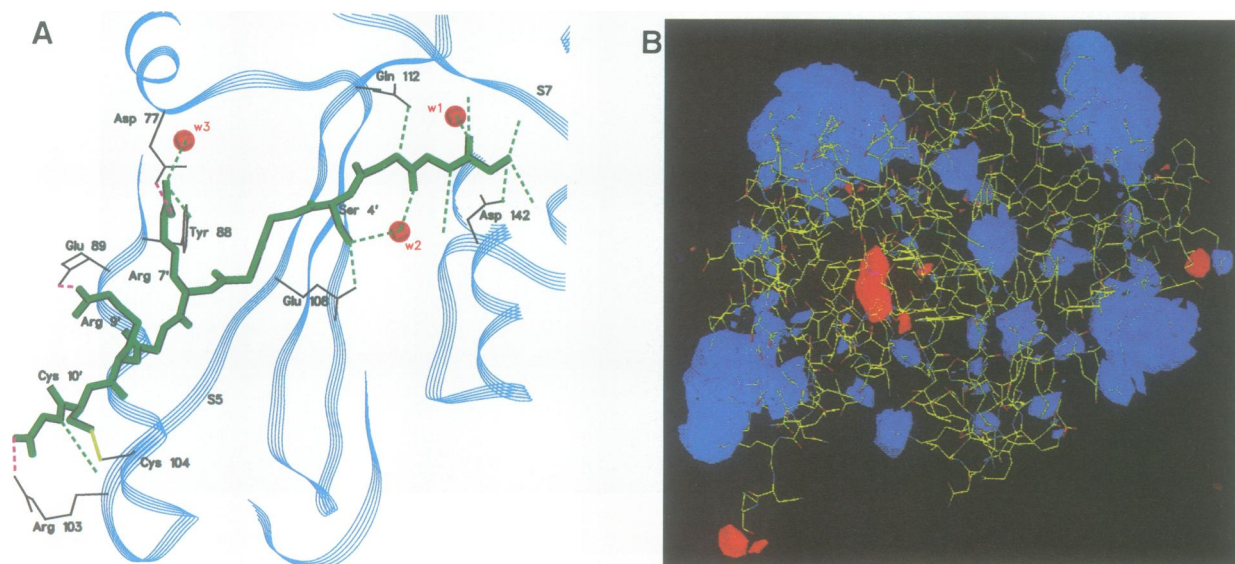


Fig. 2. The cofactors. (A) View of the detailed interaction of the pVlc peptide with the mainchain of the proteinase; (B) surface charge distribution of AVP-pVlc complex. Both points of view are similar to those in Figure 1. In (A), the pVlc peptide forms extensive hydrogen-bonding contact with AVP. Residues 1'–3' of pVlc contact several residues in and around β -strand S7; residues 4'–10' of pVlc extend the β -sheet structure of the enzyme through hydrogen bonding to β -strand S5. The pVlc peptide is colored green. AVP is represented as a blue five-stranded ribbon. AVP side chains are black. Hydrogen bonds are shown as dashed, green lines and salt bridges as dashed, red lines. The disulfide bond between pVlc Cys10' and AVP Cys104 is a solid yellow line. Water molecules are indicated by red spheres. In (B), the charge-potential map of the distribution of positive (blue) and negative (red) charges in the AVP-pVlc complex was generated with the program O (Jones *et al.*, 1991). The viewpoint is below and to the left of Figure 1.

Figure 3A shows the secondary structures of subtilisin, AVP and papain, with their catalytic residues displayed as ball-and-stick models. One can see the gross similarities: in all three there is a long, central α -helix flanked on the left by a β -sheet with several anti-parallel strands, covered eventually by a couple of helices. These similarities were recognized by eye, then the alignments shown of the C α backbones were optimized with the LSQ function in program O (Jones *et al.*, 1991) (55 residues in the AVP/subtilisin fit, 60 residues in the AVP/papain fit).

The similarities became even more interesting when, in the aligned structures, one compares the amino acids of the active-site region of papain with the amino acids in the same positions in AVP. Cys122 in AVP is in an identical position to the nucleophilic Cys25 of papain (Figure 3Ab, Ac and B). Furthermore, two other residues of AVP, His54 and Glu71, are in identical positions to those of His159 and Asn175, the two other residues of papain that constitute the charge-relay system (Blow *et al.*, 1969). In both enzymes, these two residues lie at the N- and C-terminal ends, respectively, of a β -turn- β structure. Even the gaps between these two amino acids are similar: 17 versus 16 residues, respectively.

The similarities are even more extensive: when one aligns the three active-site residues of papain and their counterparts in AVP, a fourth pair of residues comes into register (Figure 3B). These are Gln19 of papain (Drenth *et al.*, 1976), presumed to participate in formation of an oxyanion hole (Robertus *et al.*, 1972), and Gln115 of AVP. One can see in the figure that the main-chain nitrogen atoms of the two active-site Cys residues also match; in papain this atom is proposed to join with Gln19 to form the two hydrogen bonds in the oxyanion hole (Drenth *et al.*, 1976).

This remarkable juxtaposition of catalytic elements

suggests clearly that AVP must employ the same catalytic mechanism as papain (Polgar, 1974). To find these similarities among proteins with completely different folds suggests that there is either a subtly divergent or powerfully convergent evolution of these enzyme molecules to have produced this match.

Architecture and evolution of the active site

The active site must lie within the 25 Å long, bent groove that is ~8 Å wide (Figure 4), because Cys122 and His54 lie in the middle of the groove. These two amino acids are conserved among adenovirus serotypes. A 3.6 Å hydrogen bond is formed between atoms S of Cys122 and N δ of His54 (Figure 2B). This is probably a Cys–His ion pair, like the nucleophilic Cys–His ion pair in papain (Drenth *et al.*, 1971), because a thiolate anion in AVP can be titrated at pH 5.0 with dithiodipyridine (Mangel *et al.*, 1996). Glu71, probably the third member of the charge-relay system (Blow *et al.*, 1969), lies on the other side of the imidazole ring of His54 from Cys122. A 2.7 Å hydrogen bond is formed between atoms O ϵ of Glu71 and N ϵ of His54. Glu71 is replaced only by Asp among adenovirus strains. Surprisingly pVlc, which exerts powerful control on the rate of catalysis, is quite far from the active-site residues involved in catalysis: the pVlc cysteine residue, which forms a disulfide bond with Cys104 of the main chain, is 32 Å away from the active-site nucleophile Cys122. The residue of pVlc closest to the active site is Val2' whose side chain is 14.5 Å from Cys122.

Substrate modeling

We built a model for the interaction between AVP and one of its natural substrates, the cleavage site from the C-terminus of pVI, IVGL↓GV. For this model we used the chain direction found in the crystal structure of the

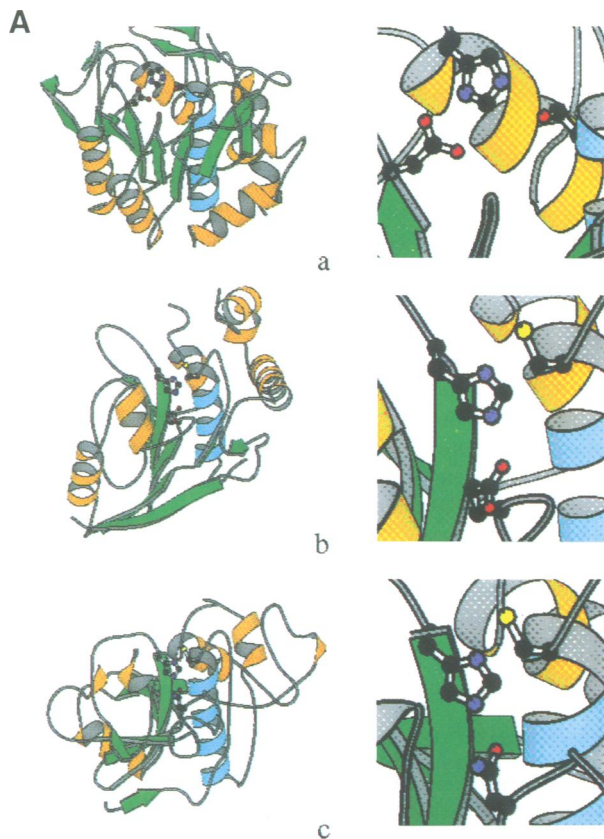
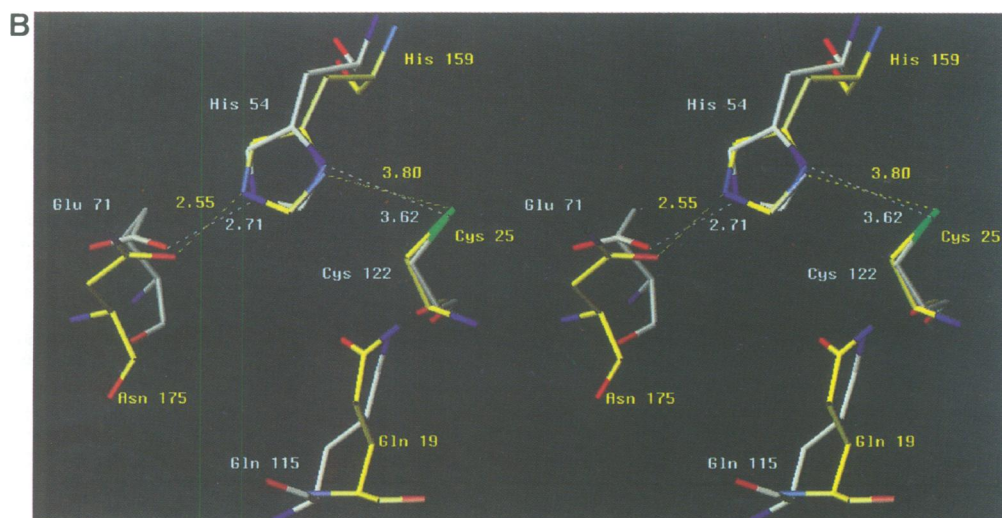


Fig. 3. (A) Overall structural alignment of (a) subtilisin, (b) AVP and (c) papain. (B) Alignment of the AVP active-site residues with those of papain. In (A), α -helices are colored yellow and β -strands are green, except for the helix colored blue in the center of each molecule. This central helix, with the β -strands immediately to its left, was the focus of the alignment. The side chains involved in catalysis are shown to the right. Magnification of each active-site region is shown to the right. Secondary structure was assigned with the program PROCHECK (Laskowski *et al.*, 1993). The figure was generated with the program MOLSCRIPT (Kraulis, 1991). In (B), the residues involved in catalysis in papain are shown after alignment of the papain molecule to fit the equivalent residues in AVP. Active-site residues and bond distances (in Å) are in white for papain and in magenta for AVP. The figure was generated using the program O (Jones *et al.*, 1991).



complex of papain with Gln-Ala-Ala-Ala-chloromethyl ketone (Drenth *et al.*, 1976). The IVGLGV peptide fit as an extended β -strand into the active-site groove. When it is arranged so that the CO group of the P₁ (Schechter and Berger, 1967) leucine residue approaches the presumed oxyanion hole, the side chains of residues P₂Gly and P₄Ile point into the groove and those of P₁Leu and P₃Val point away from the enzyme. The P₄Ile side chain lies in a pocket touching the edge of the indole ring of Trp55, and the α -carbon of the P₂Gly touches its face. With the residues P₂–P₄ in strict β -sheet configuration, three main-chain to main-chain hydrogen bonds can be formed between the substrate and the enzyme. Other H-bond donors are nearby, including the N-terminus of AVP and the conserved, buried residue Asn44.

This model provides some understanding of the specificity of this enzyme. Consensus sequences for cleavage by AVP are (M,L,I)XGX↓G or (M,L,I)XGG↓X (Webster *et al.*, 1989a,b). The main determinants of specificity are the P₂ and P₄ amino acids. We find P₂ facing a small hydrophobic pocket that can accommodate only a glycine (Figure 5). The hydrophobic pocket that P₄ occupies, formed by Trp55 (conserved) at the bottom and by the Arg48 (conserved) and Gln6 (consensus) side chains at the back, could accommodate Met, Leu or Ile. In addition, the sites for P₁ and P₃ are not inconsistent with this sequence specificity. The P₁ site lies between two hydrophobic residues on the surface, Val53 (consensus) and Leu201 (consensus). The P₃ residue can be almost any amino acid, because its side chain points away from the

enzyme. Amino acids beyond P₄ probably do not bind to the enzyme.

Discussion

The adenovirus proteinase had proven difficult to classify (Webster *et al.*, 1989a,b; McGrath *et al.*, 1996a). However, the striking similarities with papain of the three-dimensional positions of the amino acid residues involved in catalysis suggests that AVP must employ a similar catalytic mechanism. Despite the striking similarities with papain of the positions of the amino acid residues involved in catalysis, the sequential order of these amino acid residues in the polypeptide chain is different. In AVP the catalytic triad is His54, Glu71 and Cys122, whereas in papain the

order is Cys25, His159 and Asn175. Thus, if AVP is indeed a cysteine peptidase, it would be in a different class from the papain superfamily (Polgar, 1989) or the viral cysteine proteinases with chymotrypsin-like folds (Allaire *et al.*, 1994). It would belong to the subclass His/Cys (Rawlings and Barrett, 1994). Heretofore, there were four groups of enzymes with catalytic triads generated by convergent evolution towards a stable, useful active site: the eukaryotic serine proteinases, the cysteine proteinases, subtilisins, and the alpha/beta hydrolase-fold enzymes (Ollis *et al.*, 1992). Because of its unique fold, AVP must represent a fifth group.

Human adenovirus is a leading cause of infant death in third-world countries (Horwitz, 1990). The three-dimensional structure of the adenovirus proteinase will allow one to begin studies of rational drug design, e.g. against the active site or the pVIc binding site. Because this virus-coded proteinase exhibits a unique substrate specificity whose origin in structure we now know (Webster *et al.*, 1989a,b; McGrath *et al.*, 1996a), one can expect that equally specific inhibitors will abort a virus infection without interfering with normal cellular metabolism.

Materials and methods

Crystal structure determination

Details of the complete structure determination will be published elsewhere (J.Ding, W.J.McGrath, R.M.Sweet, and W.F.Mangel, in preparation).

In summary, crystals of the AVP-pVIc complex were obtained as reported elsewhere (McGrath *et al.*, 1996b). All diffraction data were measured on a MAR Research 300 mm diameter imaging-plate scanner, mounted on the θ arm of a FASTTM diffractometer at Beamline X12-C of the National Synchrotron Light Source at Brookhaven National Laboratory. Native data from one crystal were measured to 2.6 Å resolution with an X-ray wavelength of $\lambda = 1.15$ Å; derivative data from three crystals were measured at $\lambda = 1.07$ Å (at the peak of the 'white line' observed in the absorption spectrum of the heavy atoms in the crystal) to a resolution of 3 Å. The crystals had symmetry P6₁; the unit cell dimensions were $a = b = 114.2$ Å, $c = 50.1$ Å; $\alpha = \beta = 90^\circ$, $\gamma = 120^\circ$. The asymmetric unit contained one molecule with a mass of 24.5 kDa.

The structure was solved by SIRAS (single-isomorphous replacement with anomalous scattering) from a K₂PtCl₄ derivative. Heavy atoms were located with program HASSP (Terwilliger *et al.*, 1987). SIRAS phases were calculated with the PHASES package (Furey and Swaminathan, 1990). Strong phasing power led to a mean figure of

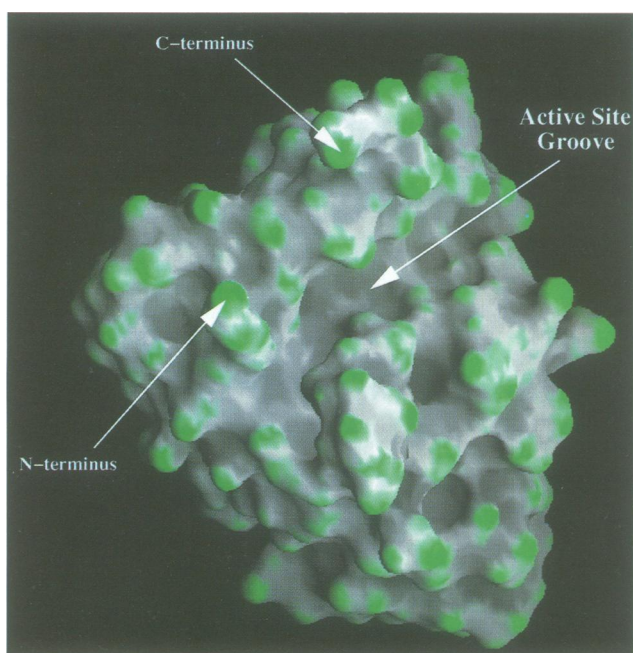


Fig. 4. Active-site groove. The groove containing the active-site residues is shown from a surface-contour map generated using the program GRASP (Nicholl and Honig, 1991). The Active Site Groove arrow is the approximate line of sight of Figure 1. The positions of the N-terminus and C-terminus are indicated by arrows. Gray areas are depressions, and green ones are sharply convex.

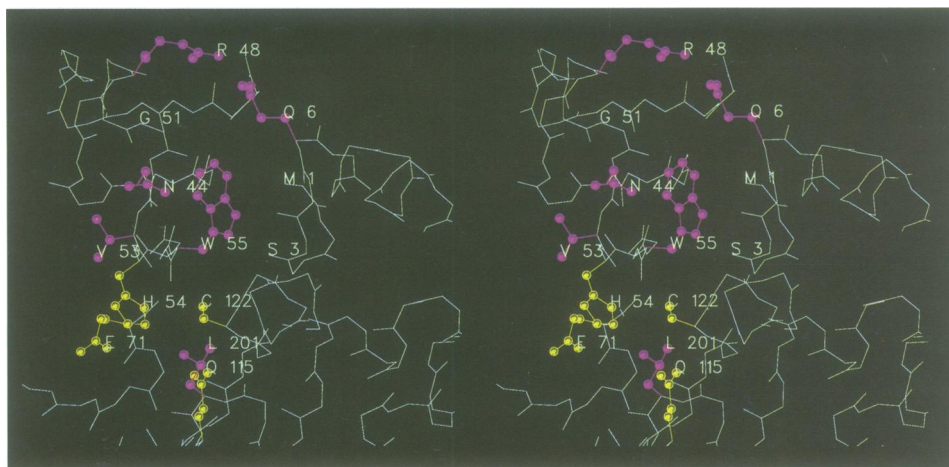


Fig. 5. View of the specificity pocket. Conserved residues potentially involved in substrate binding are shown colored. The hydrophobic pocket residues are colored magenta, active-site residues yellow, and other residues that might interact are colored green.

merit of 0.77 for 6819 reflections. Solvent flattening was performed (Wang, 1985) with PHASES. Amino acid residues were fitted with program O (Jones *et al.*, 1991). The molecular model was refined by conjugate-gradient minimization and simulated annealing with the program X-PLOR (Brünger, 1993).

Acknowledgements

We thank R.Xu for help with GRASP, X.Cheng and H.Kycia for valuable discussions, and J.Skinner, S.Sclafani, S.Williams and D.L.Toledo for technical assistance. This work was supported by National Institute of Allergy and Infectious Diseases Grant AI26049, by the Office of Health and Environmental Research of the United States Department of Energy and by the National Science Foundation. The atomic coordinates for the refined AVP-pVIc complex structure have been deposited in the Brookhaven Protein Data Bank under file name 1GJL.

References

- Allaire, M., Chernaia, M.M., Malcolm, B.A. and James, M.N.G. (1994) Picornaviral 3C cysteine proteinases have a fold similar to chymotrypsin-like serine proteinases. *Nature*, **369**, 72–76.
- Anderson, C.W. (1990) The proteinase polypeptide of adenovirus serotype-2 virions. *Virology*, **177**, 259–272.
- Anderson, C.W. (1993) Expression and purification of the adenovirus proteinase polypeptide and of a synthetic proteinase substrate. *Protein Expression Purif.*, **4**, 8–15.
- Bernstein, F.C., Koetzle, T.F., Williams, G.J.B., Meyer, E.F., Brice, M.D., Rodgers, J.R., Kennard, O., Shimanouchi, T. and Tasumi, M. (1977) The protein data bank: A computer-based archival file for macromolecular structures. *J. Mol. Biol.*, **112**, 535–542.
- Blow, D.M., Birktoft, J.J. and Hartley, B.S. (1969) Role of a buried acid group in the mechanism of action of chymotrypsin. *Nature*, **221**, 337–340.
- Brünger, A.T. (1993) X-PLOR, Version 3.1. Yale University.
- Cai, F. and Weber, J.M. (1993) Organization of the avian adenovirus genome and the structure of its endopeptidase. *Virology*, **196**, 358–362.
- Drenth, J., Jansonius, J.N., Koekoek, R. and Wolthers, B.G. (1971) The structure of papain. *Adv. Protein Chem.*, **25**, 79–115.
- Drenth, J., Kalk, K.H. and Swen, H.M. (1976) Binding of chloromethyl ketone substrate analogues to crystalline papain. *Biochemistry*, **15**, 3731–3738.
- Furey, W. and Swaminathan, S. (1990) PHASES: a package of programs for protein crystallography. *Am. Crystallogr. Assoc. Meeting Abstr.*, **PA33**, 18, 73.
- Hannan, C., Raptis, L.H., Dery, C.V. and Weber, J. (1983) Biological and structural studies with adenovirus type 2: temperature-sensitive mutant defective for uncoating. *Intervirology*, **19**, 213–223.
- Holm, L. and Sander, C. (1994) The FSSP database of structurally aligned protein fold families. *Nucleic Acids Res.*, **22**, 3600–3609.
- Horwitz, M.S. (1990) In Fields, B.N. and Knipe, D.M. (eds), *Fields Virology*. Raven Press Ltd, New York, pp. 1723–1742.
- Jones, T.A., Zou, J.Y., Cowan, S.W. and Kjeldgaard, M. (1991) Improved methods for building protein models in electron density maps and the location of errors in these models. *Acta Crystallogr.*, **A47**, 110–119.
- Kraulis, P.J. (1991) MOLSCRIPT: a program to produce both detailed and schematic plots of protein structures. *J. Appl. Crystallogr.*, **24**, 946–950.
- Laskowski, R.A., MacArthur, M.W., Moss, D.S. and Thornton, J.M. (1993) PROCHECK: a program to check the stereochemical quality of protein structures. *J. Appl. Crystallogr.*, **26**, 283–291.
- McGrath, W.J., Abola, A.P., Toledo, D.L., Brown, M.L. and Mangel, W.F. (1996a) Characterization of human adenovirus proteinase activity in disrupted virus particles. *Virology*, in press.
- McGrath, W.J., Ding, J., Sweet, R.M. and Mangel, W.F. (1996b) Crystallization of human adenovirus serotype 2 proteinase with its eleven amino acid cofactor pVIc. *J. Struct. Biol.*, in press.
- McGrath, W.J., Li, C., McWhirter, S.M., Toledo, D.L. and Mangel, W.F. (1996c) Binding to DNA by the two protein components of human adenovirus. *Biochemistry*, in press.
- Mangel, W.F., McGrath, W.J., Toledo, D.L. and Anderson, C.W. (1993) Viral DNA and a viral peptide can act as cofactors of adenovirus virion proteinase activity. *Nature*, **361**, 274–275.
- Mangel, W.F., Toledo, D.L., Brown, M.T., Martin, J.H. and McGrath, W.J. (1996) Characterization of three components of human adenovirus proteinase activity *in vitro*. *J. Biol. Chem.*, **271**, 536–543.
- Mirza, A. and Weber, J. (1980) Infectivity and uncoating of adenovirus cores. *Intervirology*, **13**, 307–311.
- Nicholl, A. and Honig, B.J. (1991) A rapid finite difference algorithm, utilizing successive over-relaxation to solve the Poisson–Boltzman equation. *J. Comp. Chem.*, **12**, 435–445.
- Ollis, D.L. *et al.* (1992) The alpha/beta hydrolase fold. *Protein Engng*, **5**, 197–211.
- Polgar, L. (1974) Mercaptide–imidazolium ion-pair: the reactive nucleophile in papain catalysis. *FEBS Lett.*, **47**, 15–18.
- Polgar, L. (1989) *Mechanisms of Protease Action*. CRC Press, Inc., Boca Raton, FL.
- Ramachandran, G.N. and Sasisekharan, V. (1968) Conformation of polypeptides and proteins. *Adv. Protein Chem.*, **23**, 283–437.
- Rawlings, N.D. and Barrett, A.J. (1994) Families of cysteine peptidases. *Methods Enzymol.*, **244**, 461–486.
- Robertus, J.D., Kraut, J., Alden, R.A. and Birktoft, J.J. (1972) Subtilisin: a stereo-chemical mechanism involving transition-state stabilization. *Biochemistry*, **11**, 4293–4303.
- Schechter, I. and Berger, A. (1967) On the size of the active site in proteases. I. Papain. *Biochem. Biophys. Res. Commun.*, **27**, 157–162.
- Terwilliger, T.C., Kim, S.-H. and Eisenberg, D. (1987) Generalized method of determining heavy-atom positions using the difference Patterson function. *Acta Crystallogr.*, **A43**, 1–5.
- Tihanyi, K., Bourbonniere, M., Houde, A., Rancourt, C. and Weber, J.M. (1993) Isolation and properties of adenovirus type 2 proteinase. *J. Biol. Chem.*, **268**, 1780–1785.
- Wang, B.C. (1985) Resolution of phase ambiguity in macromolecular crystallography. *Methods Enzymol.*, **115**, 90–112.
- Weber, J. (1976) Genetic analysis of adenovirus type 2 III. Temperature sensitivity of processing of viral proteins. *J. Virol.*, **17**, 462–471.
- Webster, A., Russell, W.C. and Kemp, G.D. (1989) Characterization of the adenovirus proteinase; development and use of a specific peptide assay. *J. Gen. Virol.*, **70**, 3215–3223.
- Webster, A., Russell, S., Talbot, P., Russell, W.C. and Kemp, G.D. (1989) Characterization of the adenovirus proteinase: substrate specificity. *J. Gen. Virol.*, **70**, 3225–3234.
- Webster, A., Hay, R.T. and Kemp, G. (1993) The adenovirus protease is activated by a virus-coded disulphide-linked peptide. *Cell*, **72**, 97–104.
- Yeh-Kai, L., Akusjarvi, G., Alestrom, P., Petterson, U., Tremblay, M. and Weber, J. (1983) Genetic identification of an endopeptidase encoded by the adenovirus genome. *J. Mol. Biol.*, **167**, 217–222.

Received on October 2, 1995; revised on November 13, 1995